SF2A 2011
G. Alecian, K. Belkacem, R. Samadi and D. Valls-Gabaud (eds)

ACES-PHARAO : MICROWAVE LINK DATA PROCESSING

F. Meynadier[1], P. Delva[1], C. Le Poncin-Lafitte[1], P. Laurent[1] and P. Wolf[1]

Abstract. The Atomic Clocks Ensemble in Space (PHARAO-ACES mission, Salomon et al. (2007)), which will be installed on board the International Space Station , uses a dedicated two-way microwave link in order to compare the timescale generated on board with those provided by many ground stations disseminated on the Earth. Phase accuracy and stability of this long range link will have a key role in the success of the PHARAO-ACES experiment.

The SYRTE is heavily involved in the design and the development of the data processing software : from theoretical modelling and numerical simulations to the development of a software prototype. Our team is working on a wide range of problems that need to be solved in order to achieve high accuracy in (almost) real time.

In this poster we present some key aspects of the measurement, as well as the current status of the software's development.

Keywords: Atomic clocks, time transfer, fundamental physics experiments.

1 The ACES mission and its microwave link

The ACES payload includes a caesium atomic clock (PHARAO) and an active hydrogen maser (SHM) which will provide a frequency reference with an expected performance around 10^{-16} in stability and accuracy. It will also include a GNSS receiver (for precise orbit determination) and two dedicated links for time comparison, one in the optical domain and the other in the microwave range.
The primary aim of the microwave link is to compare two clock signals : one is on the ground and the other is provided by the ACES payload on board of the ISS. The method that will be used is an asynchronous two way radio link with an additional downlink (at a different frequency, to derive the ionospheric delay, see fig. 2).

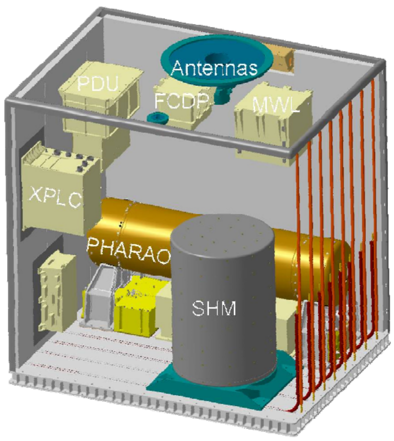

Fig. 1. The ACES payload

Time transfer is achieved by using a Pseudo-Random Noise code on the signal's carrier. Higher resolution is achieved by measuring the carrier phase of the signal. Multiple effects need to be taken into account in order to recover the clocks desynchronisation : both stations are moving during signal propagation, the troposphere and the ionosphere induce different types of delays, instrumental delays have to be calibrated and relativistic effects will come into play.

[1] LNE / Syrte – Observatoire de Paris, CNRS, UPMC Univ Paris 06, UMR8630, F-75005, Paris, France

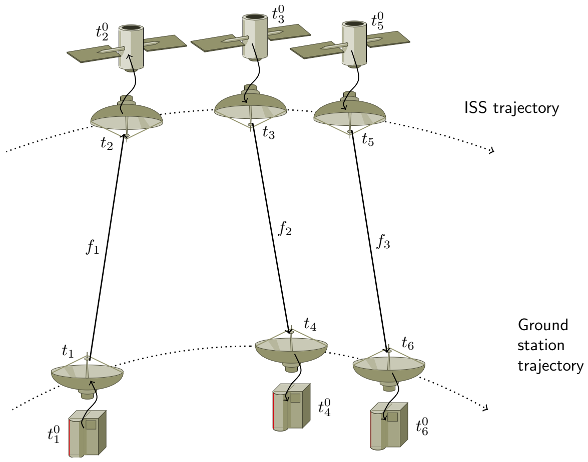

Fig. 2. The MicroWave Link (MWL) : one uplink (f_1, Ku-Band) and two downlinks (f_2, Ku and f_3, S-Band). MWL hardware developed by TimeTech GmbH. Both stations move during the signal exchange, and both have their own proper time, so a particular frame is chosen for coordinate time.

2 Two-way measurement principle

A simple one-way measurement consists in comparing the time displayed by two distant clocks, by measuring the time interval between the reception of a given tick and the generation of the same tick by the local clock. The result is a time interval $\Delta\tau = \tau_{\text{production}} - \tau_{\text{reception}}$, in the local clock's proper time. In order to recover the clocks desynchronization from this delay, one needs to model all other effects that contribute to $\Delta\tau$. The following figures exhibits the basic methods used to encode the time data on the signal, yet recovering the full resolution thanks to carrier-phase measurements.

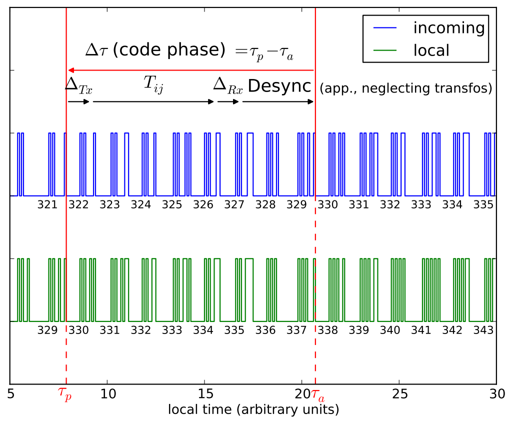

Fig. 3. Basic concept of code-phase measurement. For clarity, a simplistic encoding is used here (in reality a PRN code is used).

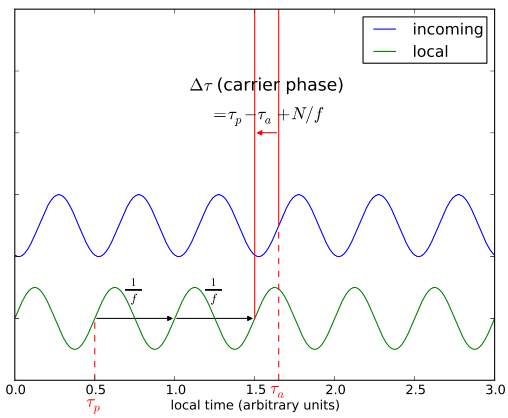

Fig. 4. Basic concept of carrier-phase measurement. For full temporal resolution is recovered, the phase ambiguity has to be resolved.

The two-way measurement aims at minimizing uncertainties by performing two symmetrical one-way measurements (i.e. one from ground to space, the other from space to ground) : when subtracting the $\Delta\tau$ obtained

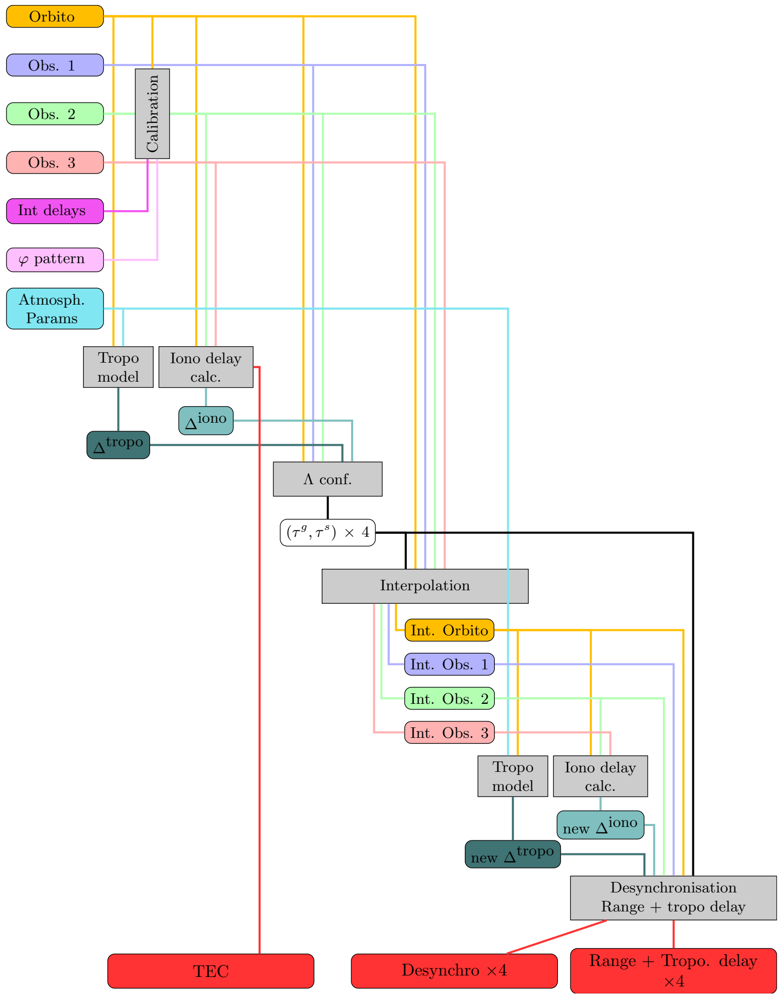

Fig. 5. Overall flowchart of the data processing software. Inputs are in the top-left corner and scientific products are at the bottom (red squares).

in each case, some major contributions (e.g. the range) cancel out at first order and the resulting desynchronisation determination is less model-dependant. A third (much lower) frequency allows to determine the ionospheric delay (and thus the total electron content).

3 Data processing software

Our team is currently developing a prototype of the data processing software. It will be used :

- as a guideline for Astrium who will implement the industrial-grade data processing in the ACES ground segment
- by our team, to achieve the highest possible accuracy in post-processing.

The core algorithm is based upon Loïc Duchayne's PhD thesis (Duchayne 2008). Its top-level flowchart is reproduced on Fig. 5

First, observables are calibrated and corrected for various systematic effects that are monitored during the mission. Then a model of the atmosphere is applied in order to correct for the delay that is induced by those layers.

One of the key aspects of this algorithm is the calculation of the Λ configuration : as downlink and uplink signals series each have their own timescale and do not coincide *a priori*, we have to interpolate one of the series in order to get a coherent measurement. The Λ configuration is a particular interpolation that ensures that the uplink signal reception coincides with the downlink signal emission (i.e. $t_2 = t_3$ on fig. 2, so the f_1 and f_2 signals form a Λ-shaped figure). This reduces the impact of the ISS's orbitography uncertainty, which is orders of magnitude less accurately known than the ground station's positions (Duchayne et al. 2009).

4 First results

We have designed and implemented the algorithm that recovers $\Delta\tau$ from raw MWL data, i.e. T_i and n_i couples as explained in this figure :

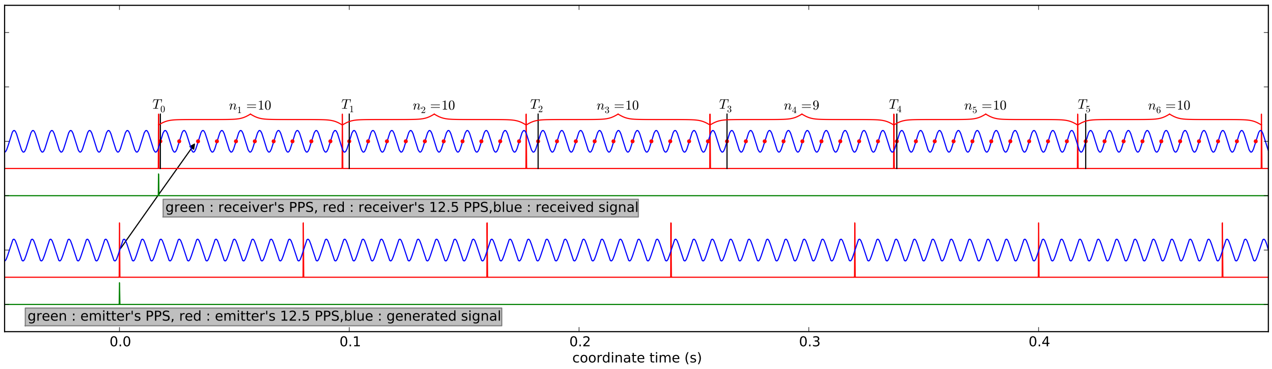

Fig. 6. A simplified diagram representing how the measurement is actually made.

Fig. 6 shows a carrier (in blue) when generated (lower part of the graph) and when received (upper part of the graph), with a slight shift and a varying frequency because of Doppler effects. Time scales (in red and green) are also different for the emitter and the receiver. Ascending zero-crossings are materialized by a red dot. For each 80 ms interval of the receiver's proper time, we get T (the date of the first zero crossing) and n, the number of zero-crossings in the previous interval.

In such a (simplified) configuration, in the receiver's time frame we get :

$$\Delta\tau(T_i) = \Delta\tau(T_{i-1}) + \frac{n_i}{f_{\mathrm{Tx}}} - (T_i - T_{i-1})$$

where f_{Tx} is the frequency of the carrier. Note that, compared to this diagram, the carrier's frequency is much higher, so it is not used directly and we get a beatnote instead : this introduces another term in the equation.

5 Simulations

Our team also develops in parallel a data simulation software. Development is as independent as possible in order to identify possible bugs or misunderstandings in the data processing software.

A first version of the simulation software is already delivering test datasets that are useful for evaluating the orders of magnitudes for the various effects that come into play. Those first batches are currently used to test and validate the first working modules of the data processing software, and will serve as "test cases" throughout the code's development.

As an illustration, fig. 7 shows a simulation of the signal's frequency based on real ISS orbitography.

References

Duchayne, L. 2008, PhD thesis, Observatoire de Paris, France

Duchayne, L., Mercier, F., & Wolf, P. 2009, A&A, 504, 653

Salomon, C., Cacciapuoti, L., & Dimarcq, N. 2007, International Journal of Modern Physics D, 16, 2511

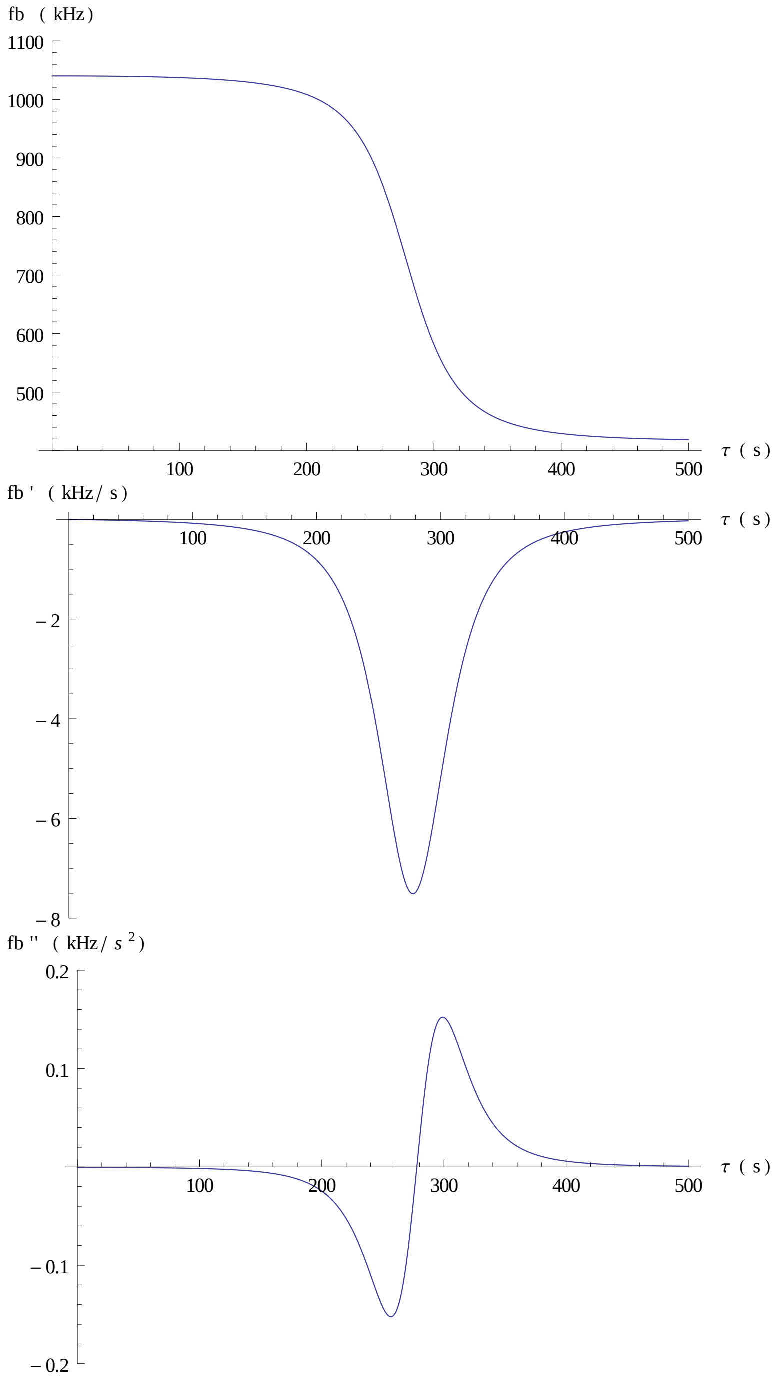

Fig. 7. The (simulated) beatnote frequency and its derivatives on board the satellite over a passage of the ISS.